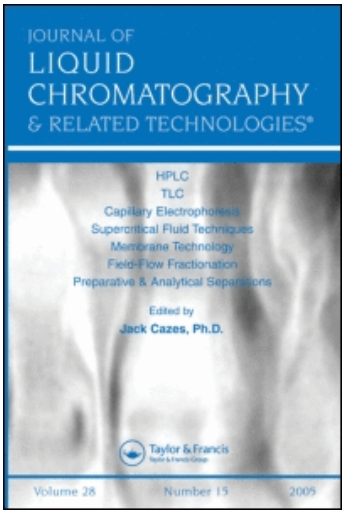

Journal of Liquid Chromatography & Related Technologies
Publication details, including instructions for authors and subscription information:
http://www.informaworld.com/smpp/title~content=t713597273

Theoretical Aspects of the Enantiomeric Resolution of Dimetallo Helicates with Different Surface Topologies on Cellulose Columns

Syma Khalid[a]; P. Mark Rodger[b]; Alison Rodger[b]
[a] Department of Biochemistry, University of Oxford, Oxford, U.K. [b] Department of Chemistry, University of Warwick, Coventry, U.K.

To cite this Article Khalid, Syma , Rodger, P. Mark and Rodger, Alison(2005) 'Theoretical Aspects of the Enantiomeric Resolution of Dimetallo Helicates with Different Surface Topologies on Cellulose Columns', Journal of Liquid Chromatography & Related Technologies, 28: 19, 2995 — 3003
To link to this Article: DOI: 10.1080/10826070500294966
URL: http://dx.doi.org/10.1080/10826070500294966

Journal of Liquid Chromatography & Related Technologies®, 28: 2995–3003, 2005

ISSN 1082-6076 print/1520-572X online
DOI: 10.1080/10826070500294966

Theoretical Aspects of the Enantiomeric Resolution of Dimetallo Helicates with Different Surface Topologies on Cellulose Columns

Syma Khalid
Department of Biochemistry, University of Oxford, Oxford, U.K.

P. Mark Rodger and Alison Rodger
Department of Chemistry, University of Warwick, Coventry, U.K.

Abstract: Cellulose has been used to separate the enantiomers of a range of dimetallo coordination compounds with different surface topologies. The compounds are all approximately cylindrical in shape, but are based on octahedral coordination at the metals and are also helical. When separation has been achieved, the first eluted enantiomer has always been proven to have a negative circular dichroism (CD) signal for its longest wavelength metal to ligand charge transfer band. In order to understand the underlying basis for the elution order, gas phase molecular dynamics and snap-shot minimisations of each enantiomer with the repeat unit of cellulose, glucose, have been undertaken. For new dimetallo helicates, it is important to have a quick assessment of the enantiomeric identity of the first eluted compound. To this end, the coupled-oscillator model of CD has been applied to relate the signs of the CD signals to the identity of the enantiomers. This correlation is consistent with crystallographic data for the first eluted enantiomer of the parent compound.

Keywords: Dimetallo helicates, Circular dichroism, Cellulose, Chromatography, Molecular modelling, Glucose

Address correspondence to Prof. Alison Rodger, Department of Chemistry, University of Warwick, Coventry, CV4 7AL, U.K.. E-mail: a.rodger@warwick.ac.uk

INTRODUCTION

A series of cationic dimetallo helicates, based on octahedral coordination at the metals by three fairly rigid tetra-dentate ligands, have been designed and synthesised at Warwick.[1–4] These helicates are of appropriate size and shape to target the major groove of DNA,[5] and upon binding they induce unusual structural changes in the DNA.[2,6] The compounds are chiral and the helicity of the complex has been found to have a significant effect on the DNA binding of the enantiomers.[6] After exhaustive searches of established resolution methodologies, we found that the enantiomers of the parent compound $[Fe_2(L_1)_3]^{4+}$ (Figure 1) can be separated using cellulose (in paper or packed in a column) with 0.02 M aqueous sodium chloride as the eluent,[7] and we have subsequently refined the mobile phases to minimise the amount of NaCl required (since this ends up in solution with the resolved enantiomers and is very difficult to remove).[8] The chromatographic behaviour of derivatives of the parent dimetallo helicate differs depending on where substituents are located. The effects, which are given in detail in reference [8], can be summarised with reference to the position labels in Figure 1 as follows. Replacing the bridging CH_2 group with O at position **A** worsens the enantiomeric separation, though does not remove it completely. Adding methyl groups on the imine bond at position **B** destroys the enantiomeric separation. Substitution at positions 3 (**C**), 5 (**E**) and 4 (**D**) of the terminal pyridine results in a small reduction in separation efficiency with their effect being in the order (**C**) < (**E**) < (**D**).

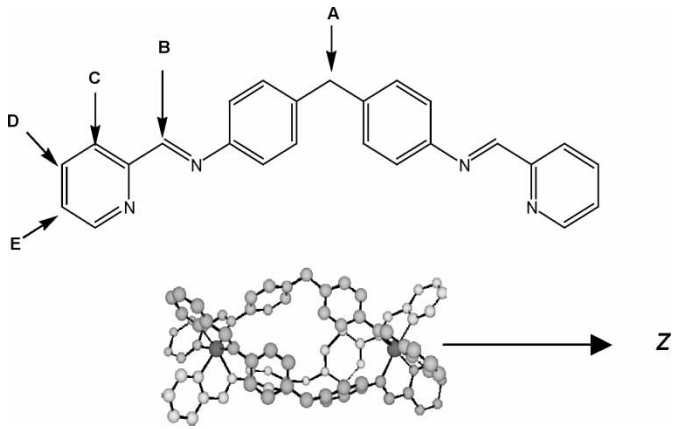

Figure 1. Ligand and dimetallohelicate structures of the parent compound $[Fe_2(L_1)_3]^{4+}$, with sites of potential substitution labelled (the substitution pattern is usually symmetric about A and is assumed to be so in this work). *z* is the 3-fold axis of the helicate.

To date, whenever chiral resolution has been achieved, the first eluting compound gives a negative circular dichroism (CD) signal in its longest wavelength band. The first eluted band of the parent compound has been shown by X-ray crystallography to be the M-helicate.[8] In order to be able to use the methodology and enantiomer assignments suggested by the circular dichroism, it is necessary to understand the basis of the molecular discrimination on the column and also the mechanistic origin of the CD signal. The aim of the work reported in this paper was, therefore, to understand why (or why not) we observed a chiral discrimination when the dimetallo helicates were eluted from a cellulose (polymer of glucose) stationary phase by examining the interactions between parent helicate and a glucose monomer, and to understand the basis of the CD spectra which could be obtained for the two enantiomers.

EXPERIMENTAL

Spectroscopy

$[Fe_2(L_1)_3]Cl_4$ was synthesised and resolved as described in reference.[6] The CD spectra were collected in 1 cm pathlength cuvettes using a Jasco J-715 spectropolarimeter, and averaged over 4 scans with response time = 1 s. Concentrations were determined using $\varepsilon_{574\,nm} = 16{,}900\,mol^{-1}\ dm^3\ cm^{-1}$ for the metal-ligand charge transfer band.[2,8] The absorption spectra were collected on a Jasco V-550 spectrometer using a 1 cm pathlength cuvette.

Computational Modelling

Models of glucose and the two helicate enantiomers were constructed. High temperature molecular dynamics (MD) simulations were performed with the cylinder frozen, while the glucose was mobile. These simulations were designed to identify likely sugar interaction sites on the cylinder. It was hoped they would provide molecular level insights into the differential cellulose binding of the two enantiomers. The configurations with the most favourable energies from the MD simulations were then energy-minimised to further optimise the geometries. The helicate coordinates were taken from the crystal structure, while glucose was constructed using the 2D sketcher module in Quanta and then energy-minimised. Compounds were modelled using the CHARMM22 all-atom force-field with modifications, so the glucose remained in the chair conformation.[10–12] Simulations were performed using DL_POLY. The conversion from CHARMM to DL_POLY force-field formats was achieved using a purpose-built program that interpreted the CHARMM prm and crd files. Simulations were performed in the *NVT* ensemble at 900 K using the Hoover thermostat with a time constant

of 0.1 ps and a time step of 2 fs. The high temperature was adopted to ensure the glucose moved around sampling all potential interaction sites.

RESULTS

Circular Dichroism Spectroscopy

Spectra for the two 'baseline separated' bands from a racemic mixture of $[Fe_2(L_1)_3]^{4+}$, loaded on a column packed with cellulose and eluted with 20 mM NaCl[6], are given in Figure 2. CD spectra for all compounds where the enantiomers could be resolved[8] give the same sign pattern, from long wavelength to shorter wavelength of $-/+/-/+/-/+$ for the first eluting enantiomer. The second eluting enantiomer has the opposite sign pattern. The labelling of the spectra in Figure 2 with M and P follows from the CD theory outlined below. This labelling has recently been confirmed for the first eluting enantiomer of the parent compound only, from a crystal structure of a crystal grown from column eluent.[8] The CD theory given below enables us to generalise the crystallographic assignment of the parent compound to all derivative compounds.

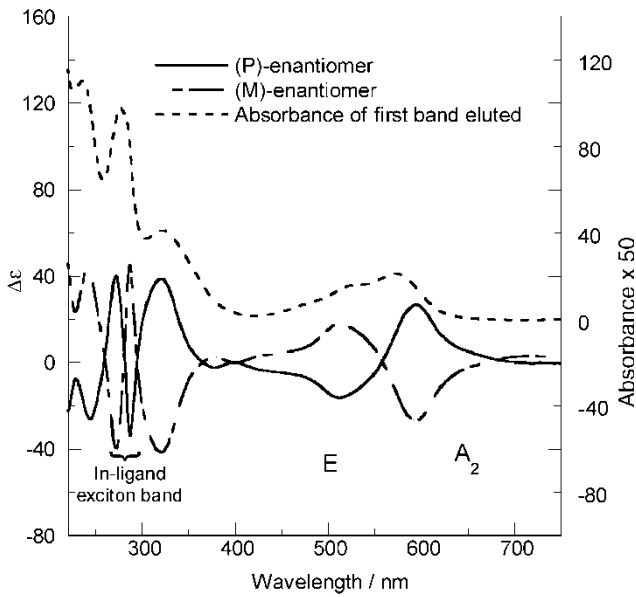

Figure 2. Absorbance of the first eluting $[Fe_2(L_1)_3]^{4+}$ band (mobile phase: 0.02 M NaCl) and the CD spectra of both bands (converted to $\Delta\varepsilon$ using concentrations determined from the absorbance magnitude and the extinction coefficient).[2,8] Absorbance (times 50) scale is on the right hand side. The spectrum labelled M is the enantiomer eluted first. Labels M and P are assigned on the basis of the CD analysis of this work.

In order to be able to use CD spectroscopy as a fast means of confirming the handedness of fractions eluted from the cellulose columns for all the dimetallo helicates, it is important to understand the origin of the signs of the bands and to be able to relate this to the handedness of the helicate. The relevant theoretical model for CD intensity of electric dipole allowed transitions in independent chromophores is the exciton coupling model.[15] For degenerate transitions, if this model is appropriate, one expects to see a characteristic exciton spectrum with a very sharp transition from negative to positive (or vice versa) signals. Such a signal is apparent in the dimetallo helicate spectra of Figure 2 centered at 280 nm. This region of the spectrum is dominated by the in-ligand transitions on the three identical chelates.

As the conjugation of the π-chelate of the dimetallo-helicates is broken at the central bridge, we can spectroscopically model the helicates as two tris-chelate metal complexes stacked vertically. The CD arising from the in-ligand couplings of single-metal tris-chelate complexes is well established.[14–16] The equations for the bimetallo tris-chelate CD can therefore be taken from the literature[15,17] after multiplying by a factor of two. As tris-chelates have $\mathbf{D}_3$ symmetry, their transitions are either polarised along the 3-fold axis, denoted z in Figure 1, or in the plane perpendicular to this. The in-ligand transitions of relevance for CD are all polarised along the chelate backbone, as the ones perpendicular to this do not give rise to a CD signal (the electron movement is in a plane, so not chiral). The z-polarised transitions are by convention labelled A_2 and the x/y-polarised, E. The CD intensity, R, for the A_2 and E polarised in-ligand bands of the P bi-metallo helicate is, therefore,

$$R\left(\frac{z}{x/y}\right) = R\left(\frac{A_2}{E}\right) = \pm\frac{\varepsilon\mu^2\rho}{\sqrt{2}\hbar} \tag{1}$$

(where the upper, in this case positive, sign refers to the upper transition polarization, namely z) with transition energies

$$\varepsilon\left(\frac{z}{x/y}\right) = \varepsilon\left(\frac{A_2}{E}\right) = \varepsilon \pm \frac{\mu^2}{12\sqrt{3}\rho^3} \tag{2}$$

where ε is the energy of the unperturbed transition, μ is the magnitude of its transition dipole moment, and ρ is the distance from the metal to the centre of a chelating part of the ligand. As $R(z)$ is the z (or A_2) polarized CD that results from the in-phase coupling of the transition moments on the three ligands, the A_2 band occurs at the higher energy (shorter wavelength). It is positive in sign for the P-enantiomer. $R(x/y)$ by way of contrast results from the out-of-phase coupling of the transition moments and is opposite in sign from $R(z)$. The energy ordering is the same for the M-enantiomer, but the sign pattern is inverted. This lets us identify the handedness of enantiomers eluting from the column: if the higher energy (shorter wavelength) band of the 280 nm

couplet is positive, then the complex is the P enantiomer. Thus, the second eluting enantiomer is P.

The other bands in the spectrum are less clearly excitonic in nature, arising as they do from a complicated overlay of different metal ligand charge transfer (MLCT) and in-ligand bands. However, it is convenient to have an empirical rule based only on the longest wavelength CD band. To this end, it is necessary to understand the longest wavelength MLCT band CD. The dilemma here is that the available data on transition polarisations of long wavelength charge transfer transitions for low spin iron(II) and ruthenium(II) (including our own stretched film *LD* assignments of transition polarisations in Fe_2L_3)[16] show significantly more (>90%) E than A_2 intensity of the long wavelength end of the absorbance spectrum, but the CD spectra show similar magnitude positive and negative bands, which, assuming the CD signals arises from a similar mechanism, requires both A_2 and E absorption intensities to be of similar magnitudes.

The dilemma is resolved by realising that E-polarised MLCT transitions occurring from an Fe metal *d* orbital to the middle of a ligand π^* orbital[18] will have significant absorbance intensity, but will involve planar electron movement, and thus will not give rise to a CD signal MLCT transitions into long axis polarised π^* states will give rise to both E and A_2 MLCT absorbance intensity, both of which will have a helical twist and give rise to a CD signal. The net effect will be that the absorbance spectrum is dominated by E polarised transitions in regions where there are short-axis polarised MLCT bands, whereas the CD spectrum will have similar magnitude contributions from the two polarisations in accordance with the experimental observation. Using the enantiomeric assignment made using the 280 nm in-ligand band (for which we also know the energy ordering of components, see above), we conclude that the longest wavelength P enantiomer MLCT CD, which is positive in sign, is due to an A_2 transition (Equation (1)). The longest wavelength band for all helicates is thus A_2, and can be used to assign the handedness of the helicates. For all the compounds investigated to date,[8] if enantiomeric resolution occurs, the first eluting enantiomer has a negative CD sign, M.

Modelling

The molecular modelling of glucose, the cellulose monomer, interacting with the two enantiomers of $[Fe_2(L_1)_3]^{4+}$ revealed three sites with more favourable interaction energies. Two of these involved the sugar being near one of the metal centres and the other was near the bridging CH_2 group (Figure 3). The interaction energies of each enantiomer of $[Fe_2(L_1)_3]^{4+}$ with a sugar in each of these sites are given in Table 1. Interaction energy = total configurational energy − configurational energy of glucose (the helicate is frozen so only contributes to the non-bonded energy). Simulations were also performed for the helicate where the CH_2 bridge is replaced by O.

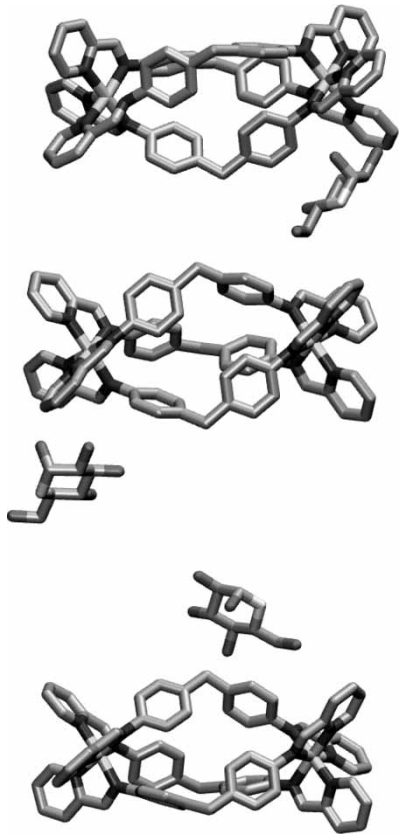

Figure 3. Site 1 (top), site 2 (middle) and site 3 (bottom). Hydrogens have been omitted for clarity. The sites are shown for the M enantiomer.

In each of the three interactions sites on $[Fe_2(L_1)_3]^{4+}$ favoured by the glucose, the interaction is strongest between the P-enantiomer and the glucose, meaning that the M-enantiomer is expected to come off a column first—as it indeed does. It follows that, when sites 1 and 2 are blocked by, e.g., a methyl substituent on the immine bond, the resolution between the enantiomers is expected to be reduced. In practice,[8] loss of sites 1 and 2 is sufficient to completely remove the enantiomeric resolution. The calculations suggest, however, that with great care and collecting beginnings and ends of fractions, some degree of resolution might be achieved.

The overall strongest interaction for the glucose with the P-enantiomer of $[Fe_2(L_1)_3]^{4+}$ is at the site nearest the bridging group (site 3, Fig. 3). Contrary to our expectations (given the charged nature of the metallo-helicate), when the bridging CH_2 was replaced by the potentially H-bonding O atom the interaction of the glucose with site 3 became less attractive, and it always

Table 1. Interaction energies of each enantiomer of $[Fe_2(L_1)_3]^{4+}$ and the analogous compound where the CH_2 bridge is replaced by O (denoted O in the table) with a glucose molecule in each of the 3 favourable sites. Site 3 is near the bridging CH_2 or O

	Site 1	Interaction energy (kcal mol^{-1})	Site 2	Interaction energy (kcal mol^{-1})	Site 3	Interaction energy (kcal mol^{-1})
CH_2	P	−9.0	P	−8.4	P	−11.0
CH_2	M	−7.9	M	−7.1	M	−6.2
O	P	−8.9	P	−8.4	P	—
O	M	−7.9	M	−7.1	M	—

migrated to sites 1 or 2. The experimental consequence of this would be predicted to be that the discrimination between the enantiomers is reduced and their residence time on the column is shortened. This is indeed the case. The enantiomeric resolution of the O-bridged helicates is significantly smaller than that of the parent compound,[8] and both O-bridged enantiomers have larger R_f values (distance moved by analyte divided by distance moved by solvent front) on cellulose paper than the corresponding CH_2 compound.[8]

CONCLUSIONS

From the analysis of the CD of the in-ligand exciton band and the longest wavelength MLCT region of the spectrum, we can conclude that CD can be used to assign the handedness of the di-iron triple helicates. A negative long wavelength band corresponds to the M-enantiomer. To date, from the data in reference [8], we conclude here that it is always the M-enantiomer which elutes first from cellulose and the P-enantiomer which elutes second, whenever any resolution is achieved. For other metals initial consideration of the in-ligand region of the spectrum would be necessary before establishing such a rule. Molecular modelling of glucose monomers and both M and P helicates has been used to understand why the elution occurs in this way. In general terms, P interacts more favourably with glucose so is retained on a column. Much of this discrimination arises from interaction near the metal atoms. It follows from this, that when this site is filled up with a substituent on the immine, such as CH_3, then the chiral resolution is reduced or removed. The origin of lower resolution when the bridging atom is changed from CH_2 to the electronegative O arises, somewhat surprisingly, from the fact that the H-bonding glucose does not interact as favourably with the O-bridged site as with the other sites near the metal. This then reduces the time the helicates spend on the column and reduces the discrimination between the enantiomers, as there is no contribution from the bridging site.

REFERENCES

1. Hannon, M.J.; Painting, C.L.; Jackson, A.; Hamblin, J.; Errington, W. Chem. Commun. **1997**, 1807–1808.
2. Rodger, A.; Sanders, K.J.; Hannon, M.J.; Meistermann, I.; Parkinson, A.; Vidler, D.S.; Haworth, I.S. Chirality **2000**, *12*, 221–236.
3. Hannon, M.J.; Painting, C.L.; Alcock, N.W. Chem. Commun. **1999**, 2023–2024.
4. Uerpmann, C.; Malina, J.; Pascu, M.; Clarkson, G.J.; Moreno, V.; Rodger, A.; Grandas, A.; Hannon, M.J. Chem. Eur. J. **2005**.
5. Hannon, M.J.; Moreno, V.; Prieto, M.J.; Molderheim, E.; Sletten, E.; Meistermann, I.; Isaac, C.J.; Sanders, K.J.; Rodger, A. Angew. Chem. Int. Ed. **2001**, *40* (5), 880–884.
6. Meistermann, I.; Moreno, V.; Prieto, M.J.; Molderheim, E.; Sletten, E.; Khalid, S.; Rodger, P.M.; Peberdy, J.C.; Isaac, C.J.; Rodger, A.; Hannon, M.J. Proc. Natl. Acad. Sci. **2002**, *99* (8), 5069–5074.
7. Hannon, M.J.; Meistermann, I.; Isaac, C.J.; Blomme, C.; Aldrich-Wright, J.R.; Rodger, A. Chem. Commun. **2001**, 1078–1079.
8. Peberdy, J.C.; Reudegger, V.; Kerchoffs, J.; Rodger, A.; Hannon, M.J. Submitted.
9. Accelrys. In *QUANTA, Accelrys*; San Diego, CA, 2000.
10. MacKerell, A.D., Jr.; Bashford, D.; Bellot, M.; Dunbrack, R.L., Jr.; Evanseck, J.D.; Field, M.J.; Fischer, S.; Gao, J.; Guo, H.; Ha, S.; Joseph-McCarthy, D.; Kuchnir, L.; Kuczera, K.; Lau, F.T.K.; Mattos, C.; Michnik, S.; Ngo, T.; Nguyen, D.T.; Prodhom, B.; Reiher, W.E., III; Roux, B.; Schlenkrich, M.; Smith, J.C.; Stote, R.; Straub, J.; Watanabe, M.; Wiorkiewicz-Kuczera, J.; Yin, D.; Karplus, M. J. Phys. Chem. B. **1998**, *102*, 3586–3616.
11. Astley, T.; Birch, G.G.; Drew, M.G.B.; Rodger, P.M. J. Phys. Chem. A **1999**, *103*, 5080–5090.
12. Astley, T.; Birch, G.G.; Drew, M.G.B.; Rodger, P.M.; Wilden, G.R.H. Food Chemistry **1996**, *56*, 231–240.
13. Smith, W.; Forester, T.R.J. Mol. Graphics **1996**, *14*, 136–141.
14. Bosnich, B. Acc. Chem. Res. **1969**, *2*, 266–273.
15. Rodger, A.; Nordén, B. *Circular Dichroism and Linear Dichroism*; Oxford University Press: Oxford, 1997.
16. Holder, E.; Trapp, G.; Grimm, G.; Schurig, V.; Lindner, E. Tet. Asym. **2002**, *13*, 2673–2678.
17. Armstrong, D.W.; DeMond, W.; Czech, B.P. Anal. Chem. **1985**, *57*, 481–484.
18. Green, J.M.; Jones, R.; Harrison, R.D.; Edwards, D.S.; Glajch, J.L. J. Chromatogr. **1993**, *635*, 203–209.

Received June 1, 2005
Accepted June 30, 2005
Manuscript 6667